

## REMARKS

Favorable reconsideration is respectfully requested.

Upon entry of the above amendment, the claims will be 1, 3, 7 to 14 and 17 to 26 with claims 20 to 26 being withdrawn from consideration.

The above amendment is responsive to points set forth in the Official Action.

In Official Action, page 3, Claims 1, 3, 7-14 and 16 have been rejected under 35 U.S.C. 103(a) as being unpatentable over PCT Publication No. WO 94/09055 (PCT '055) in view of PCT Publication No. WO 00/08087 (PCT '087) and Mas et al. article.

As for PCT '055 and PCT '087, Applicants reiterate their comments dated January 22, 2004.

With regard to Mas et al. article, the rejection states that it is unclear whether Japanese priority applications 2001-31763 (February 8, 2001), 2001-53204 (February 27, 2001) and 2001-66440 (March 9, 2001) antedate the reference since the month and day of publication are not indicated in the abstract.

Attached herewith is a copy of Mas et al. article. As is seen on the left upper portion of its cover page, this Mas et al. article was published on August 30, 2001, which is later than the filing dates of the above-mentioned three Japanese priority applications.

Therefore the Mas et al. article cannot be prior art against the present application.

Verified English translations of the above-mentioned three Japanese priority applications are enclosed.

In Official Action, page 4, the rejection states, "...Claims 1,3 and 7-14 requiring as much as 5 parts by weight of zinc triflate without the affirmative inclusion of water is not accorded the earlier filing dates of Japanese priority documents."

In Official Action, page 5, the rejection further states:

"...the evidence is not commensurate in scope with the claimed proportion range of from 0.01 to 5 parts by weight of zinc triflate which are orders of magnitude broader than the tested amounts of 0.2, 0.5, 1.0, 1.5 and 3 parts by weight."

In reply the above amendment to Claim 1 is fully supported by Applicants' Japanese priority documents e.g. 2001-31763 at page 4, lines 9 and 10 of the English

translation, 2001-66440 at page 5, lines 15 to 21 and 2001-53204 at page 11, lines 7 and 8.

Claims 17-19 have also been rejected under 35 U.S.C. 103(a) as being unpatentable over PCT '087 and PCT '055 in view of Kitabatake et al. U.S. Patent No. 6,369,133 and Japanese Patent No. 4-359075.

As for Kitabatake et al. and JP No. 4-359075 please see Applicants comments in the response of January 22, 2004.

Incidentally, the U.S. filing date (March 2, 2001) of Kitabatake et al. is later than the filing dates (February 8, 2001 and February 27, 2001) of the first two priority applications. Therefore, the English translations of the Japanese priority applications also antedate Kitabatake.

No further issues remaining, allowance of this application is respectfully requested.

If the Examiner has any comments or proposals for expediting prosecution, please contact undersigned at the telephone number below.

Respectfully submitted,

Hisashi ISAKA et al.

THE COMMISSIONER IS AUTHORIZED  
TO CHARGE ANY DEFICIENCY IN THE  
FEES FOR THIS PAPER TO DEPOSIT  
ACCOUNT NO. 23-0975

By: Matthew M. Jacob  
Matthew M. Jacob  
Registration No. 25,154  
Attorney for Applicants

MJ/kes  
Washington, D.C. 20006-1021  
Telephone (202) 721-8200  
Facsimile (202) 721-8250  
May 17, 2004

This Page Is Inserted by IFW Operations  
and is not a part of the Official Record

## **BEST AVAILABLE IMAGES**

Defective images within this document are accurate representations of the original documents submitted by the applicant.

Defects in the images may include (but are not limited to):

- BLACK BORDERS
- TEXT CUT OFF AT TOP, BOTTOM OR SIDES
- FADED TEXT
- ILLEGIBLE TEXT
- SKEWED/SLANTED IMAGES
- COLORED PHOTOS
- BLACK OR VERY BLACK AND WHITE DARK PHOTOS
- GRAY SCALE DOCUMENTS

**IMAGES ARE BEST AVAILABLE COPY.**

**As rescanning documents *will not* correct images,  
please do not report the images to the  
Image Problem Mailbox.**

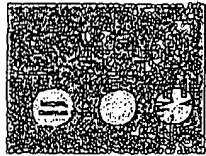
2483-2653

Vol. 202

August 30, 2001

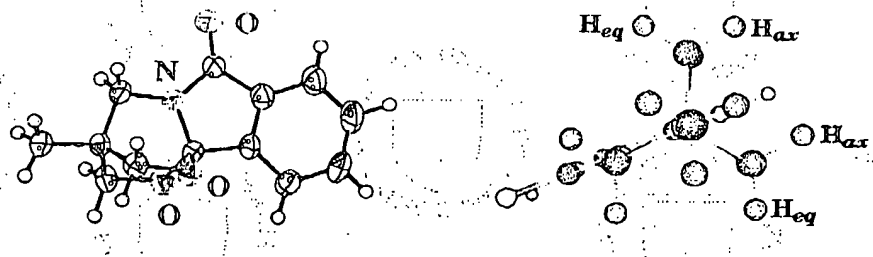
123

# Macromolecular Chemistry and Physics

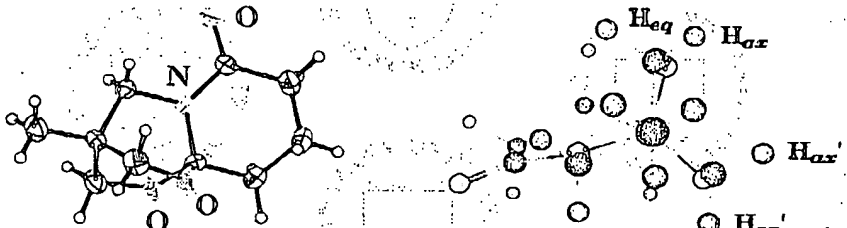
Macromolecular  
Bioscience

Macromolecular  
Bioscience

Macromolecular  
Bioscience



Polymerizable and  
Non-Polymerizable Bicyclic Acetals



Founded by Hermann Staudinger

関西ペイント(株)



600261297

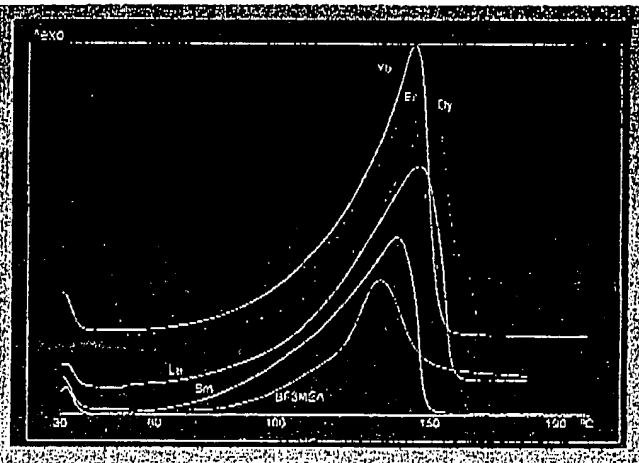


WILEY  
Interscience®  
This journal is online  
www.interscience.wiley.com

WILEY-VCH

Phenylglycidyl ether and several metal salts in various proportions have been used. The triflates salts were compared with the conventional  $\text{BF}_3$ -MEA system. The processes have been kinetically evaluated by isoconversional analysis, time and temperature predictions have been made. Their mechanical properties have been evaluated by dynamic mechanical thermal analysis (DMTA).

DSC plots of 3,4-epoxycyclohexylmethyl 3,4-epoxycyclohexane carboxylate containing 1 phr of different lanthanide triflates and 1 phr of  $\text{BF}_3$ -MEA as catalysts.



## Study of Lanthanide Triflates as New Curing Initiators for Cycloaliphatic Epoxy Resins

Christina Mas,<sup>1</sup> Angels Serra,<sup>\* 1</sup> Ana Mantecón,<sup>1</sup> Josep M. Salla,<sup>2</sup> Xavier Ramis<sup>2</sup>

<sup>1</sup> Departament de Q. Analítica i Q. Orgànica. Universitat Rovira i Virgili. Plaça Imperial Tàrraco 1, 43005 Tarragona, Spain  
E-mail: serra@quimica.urv.es

<sup>2</sup> Departament de Màquines i Motors Tèrmics. Universitat Politècnica de Catalunya, Av. Diagonal 647, 08028 Barcelona, Spain

### Introduction

Catalysts are important in polymerization processes because they decrease the activation energies and accelerate the reaction. They can be stimulated by heating or photoirradiation but, from the practical point of view, heating is the easier option; homogeneous heating of reaction mixtures can be achieved without difficulty.<sup>[1]</sup> Moreover, elementary reactions are accelerated and the viscosity of the reaction mixture decreases. This shortens the reaction time, especially for systems in which the curing rate is diffusion-determined.

Among the new thermal initiators, sulfonium, ammonium, phosphonium and hydrazinium salts are described as latent initiators that can polymerize epoxide monomers by a cationic mechanism. The order of reactivity of the cationic salts also depends on the nature of the counter anions;  $\text{Cl}^-$ ,  $\text{BF}_4^-$ ,  $\text{SbF}_6^-$ ,  $\text{PF}_6^-$  being the more active the less nucleophilic. Low nucleophilicity minimizes or prevents the reaction of the growing chain with the anion.

It is well documented<sup>[2]</sup> that the hard character and great oxophilicity of lanthanide compounds is highly improved in the case of lanthanide triflates because of the

electron-withdrawing capacity of the anionic group, which can coordinate to the epoxide oxygens leading and weaken the C—O bond. The lanthanide trifluoromethanesulfonate salts studied in this paper contain an anion with an extremely poor nucleophilicity. Therefore, very low proportions of chain-end processes are expected. Moreover, this anion is more stable than  $\text{PF}_6^-$  since it decomposes to produce  $\text{PF}_5$  and  $\text{F}^-$ , which stops the chain from growing.

The most widely used cationic polymerization catalysts in the field of epoxy technology have been the  $\text{BF}_3$ /amine system. Epoxy formulations catalyzed by these compounds are relatively stable at room temperature and cure rapidly when exposed to high temperature. However, these amine complexes are not only generally hygroscopic, but also the electrical properties of cured resins tend to deteriorate at high temperature and high humidity. Unlike  $\text{BF}_3$ /amine complexes, lanthanide triflates are stable even in aqueous media and have a strong Lewis acid character.

Cycloaliphatic epoxy resins have low viscosity and their curing resins are generally characterized by high

deflection temperature (HDT) and excellent electrical properties but are poor in mechanical elongation and toughness because of their compact molecular structure. Cycloaliphatic epoxy resins are more reactive than glycidyl resins in cationic polymerization, since epoxy groups on cycloaliphatic moieties have a higher electronic density on the oxygen atom and therefore they preferably polymerize by this mechanism.

In a previous paper,<sup>[3]</sup> we studied the crosslinking of DGEBA commercial resins with lanthanide triflates as initiators in order to test their effectiveness. We concluded that lanthanide triflates are stable and able to cure epoxy resins at moderate temperature even in very small proportions. To find out whether these catalysts are effective for cycloaliphatic epoxy resins, even when an ester group with Lewis basic character is present in their structure, we have made a kinetic study by the isoconversional method. Similarly, the materials have been characterized by thermogravimetric analysis (TGA) and dynamic mechanical analysis (DMTA) to evaluate their properties.

## Experimental Part

### Materials

3,4-Epoxycyclohexylmethyl 3,4-epoxycyclohexane carboxylate (Epoxy equiv. = 126 g/eq) (ALDRICH) was used as received.

Ytterbium(III), samarium(III), erbium(III), and dysprosium(III) trifluoromethanesulfonates (ALDRICH) and lanthanum(III) trifluoromethanesulfonate (ALFA AESAR) were used without purification.

Solvents were purified by standard methods.

The samples were prepared by dissolving the resin in methanol and mixing it with the required amount of the selected triflate salt previously dissolved in dichloromethane. The solvents were evaporated at room temperature under vacuum.

### Characterization and Measurements

Calorimetric studies were carried out on a Mettler DSC-821e thermal analyzer in covered Al pans under N<sub>2</sub> at various heating rates (5–20 °C/min). The calorimeter was calibrated using an indium standard (heat flow calibration) and an indium-lead-zinc standard (temperature calibration). The resin or the mixture of about 5 mg of known weight of the epoxy and the suitable amount of initiator was put into an aluminium pan. The kinetics of curing epoxy resins were evaluated using the kinetic software STAR of Mettler-Toledo.

Thermogravimetric analyses were carried out with a Perkin Elmer TGA-7 system in N<sub>2</sub> at 20 °C/min.

A Rheometrics instruments dynamic mechanical thermal analyzer (DMTA) PL-DMTA MK3 was used to measure the storage modulus (E') and the loss factor (tan δ) of the cured epoxy samples with a post-cured treatment in an oven at 180 °C for 24 h. DMTA was used in the single cantilever bending mode at a frequency of 1 Hz. The width of the pris-

matic samples ranged from 3 to 5 mm and their support spans were 5 mm. The thickness of the specimen ranged from 1.3 to 1.4 mm. Dynamic scans were performed from –150 °C to 200 °C at a heating rate of 2 °C/min.

## Results and Discussion

Initiators have a great influence on the properties of the thermosetting materials. Mechanical characteristics, long-term stability, chemical resistance and electrical properties vary with the nature of the crosslinking reaction that depends on the type of catalyst.

Cycloaliphatic epoxides react differently to glycidyl ones. Their order of reactivity with carboxylic acids, alcohols and amines is opposite to that of the glycidyl epoxides.<sup>[4,5]</sup> Similarly, it is known that cycloaliphatic epoxides have a higher reactivity with cationic hardeners than glycidyl ones.<sup>[6]</sup> Cycloaliphatic resins have been used in cationic-UV cure coatings,<sup>[7]</sup> leading to homopolymerization initiated by a photolytically generated superacid. These resins have also been crosslinked with cationic hardeners like BF<sub>3</sub> · MEA,<sup>[8]</sup> which have latent characteristics. This system has also been widely applied to the DGEBA resin, leading to networks with good mechanical strength.<sup>[9]</sup> However, the thermosetting materials obtained from cycloaliphatic epoxy resins and this initiator does not have good thermal stability and electrical properties at very high temperatures. Moreover, BF<sub>3</sub> · MEA is difficult to handle as it is sensitive to humidity and causes corrosion problems during processing.<sup>[3]</sup>

In a previous paper<sup>[3]</sup> we described the kinetic study of DGEBA epoxy resin with lanthanide triflates, a new series of Lewis acid catalysis. The thermosetting materials had good mechanical and thermal properties. Lanthanide triflates are stable at room temperature and soluble in organic compounds. The curing agent in the resin should be soluble because heterogeneous dispersions are liable to settle down or agglomerate during storage. It is also useful for manufacturing purposes to be able to form a solution containing both an epoxide and a curing agent.

In this paper we have studied the curing of cycloaliphatic epoxy resins with lanthanide triflates in order to overcome the above difficulties caused by the BF<sub>3</sub> · MEA system.

The kinetic characterization of the new system is important not only to understand the structure-properties relationship better, but also to optimize the process conditions and predict the behavior of the system at different temperatures and times of curing.

Differential scanning calorimetry (DSC) is very useful for studying thermal characteristics and kinetic parameters. Therefore, samples of cycloaliphatic epoxy resin (3,4-epoxycyclohexylmethyl 3,4-epoxycyclohexane carboxylate) containing the required amounts of lanthanum,

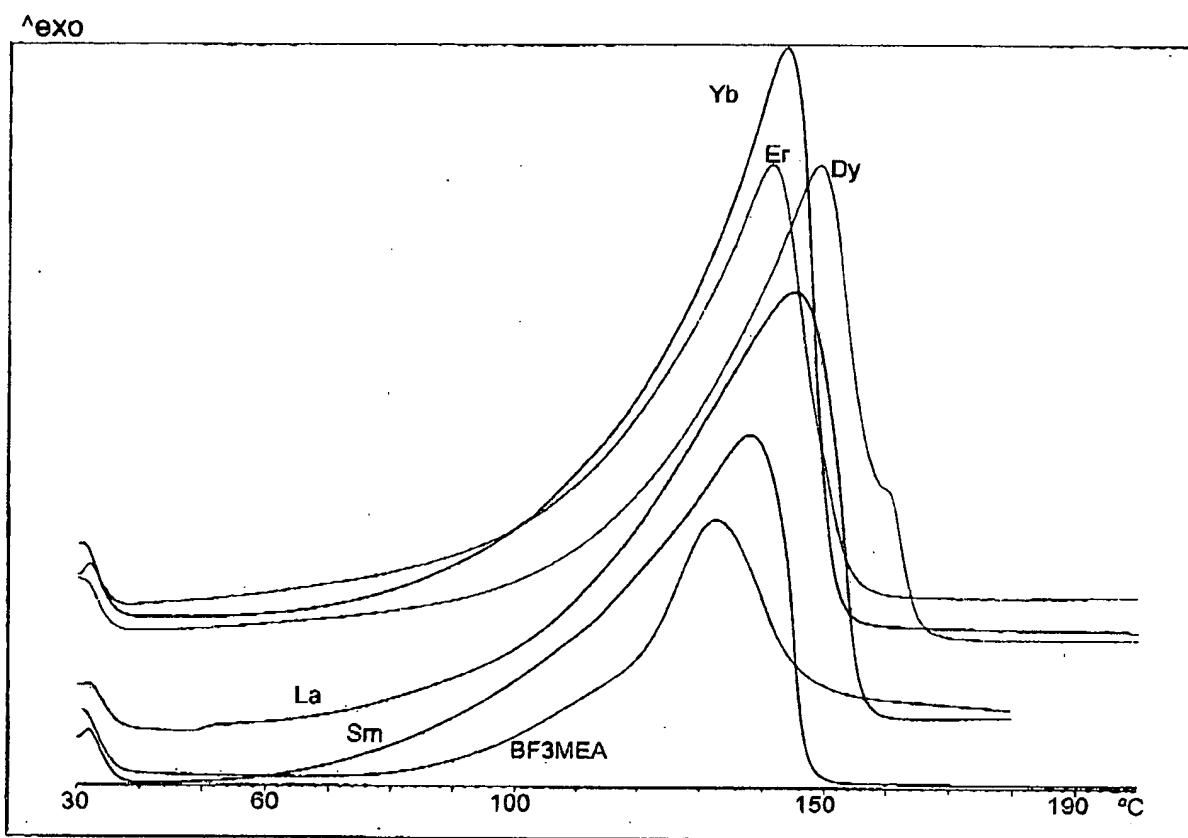


Figure 1. DSC plots of 3,4-epoxycyclohexylmethyl 3,4-epoxycyclohexane carboxylate containing 1 phr of different lanthanide triflates and 3 phr of  $\text{BF}_3 \cdot \text{MEA}$  as catalysts.

yterbium, samarium, dysprosium or erbium triflates were submitted to dynamic heating to test their behavior. Different amounts of the catalysts were used to find the most suitable percentage of hardener.

For comparison studies,  $\text{BF}_3 \cdot \text{MEA}$  was also studied at the same conditions, since it leads to a similar structure of the network. Figure 1 shows the DSC curves of the samples containing 1 phr (one part of catalyst per hundred of resin) of each lanthanide salt. The shapes of the curves are very similar; there are slight differences at temperatures before the maximum of the peak. The same figure shows the curve corresponding to the curing with 3 phr of  $\text{BF}_3 \cdot \text{MEA}$ . It must be mentioned that 1 phr of this catalyst is not sufficient to achieve the complete cure of the resin.

Table 1 shows the values obtained from these curves. The temperature at which the crosslinking begins can be evaluated from the onset temperature. The onset temperatures of samarium and lanthanum are very close and slightly lower than the others. The temperatures of the maximum of the peak do not show great differences but samarium triflate has the lowest value. The enthalpies of the curing are evaluated by integrating the exothermic peak. Dysprosium triflate thus gives a more exothermic

Table 1. DSC data obtained from dynamic scans of 3,4-epoxycyclohexylmethyl 3,4-epoxycyclohexane carboxylate containing 1 phr of different lanthanide triflates, different amounts of lanthanum triflate and 3 phr of  $\text{BF}_3 \cdot \text{MEA}$  as catalysts.

| Initiator                 | Init. percent.<br>phr | $\Delta H$<br>kJ/mol | $T_{\text{onset}}$<br>°C | $T_{\text{max}}$<br>°C | $T_g$<br>°C |
|---------------------------|-----------------------|----------------------|--------------------------|------------------------|-------------|
| $\text{Yb}(\text{OTf})_3$ | 1                     | 123                  | 117                      | 146                    | 56          |
| $\text{Sm}(\text{OTf})_3$ | 1                     | 100                  | 100                      | 139                    | 105         |
| $\text{Dy}(\text{OTf})_3$ | 1                     | 144                  | 120                      | 151                    | 91          |
| $\text{Er}(\text{OTf})_3$ | 1                     | 117                  | 114                      | 143                    | 88          |
| $\text{La}(\text{OTf})_3$ | 1                     | 118                  | 102                      | 146                    | 106         |
| $\text{La}(\text{OTf})_3$ | 1.5                   | 65                   | 82                       | 121                    | -           |
| $\text{La}(\text{OTf})_3$ | 0.5                   | 104                  | 115                      | 157                    | -           |
| $\text{BF}_3\text{MEA}$   | 3                     | 38                   | 117                      | 133                    | -           |

curing reaction but does not lead to the highest  $T_g$  value. In the most cases, the viscosity of the sample increases during the sample preparation process and some heat can be evolved. Therefore, a slight curing could take place before the curves are recorded. This makes the evaluation of curing enthalpies unreliable and it is therefore impossible to establish an accurate relationship between the enthalpies and the  $T_g$ 's of the cured materials. Likewise, the cationic mechanism of the reaction can lead to the

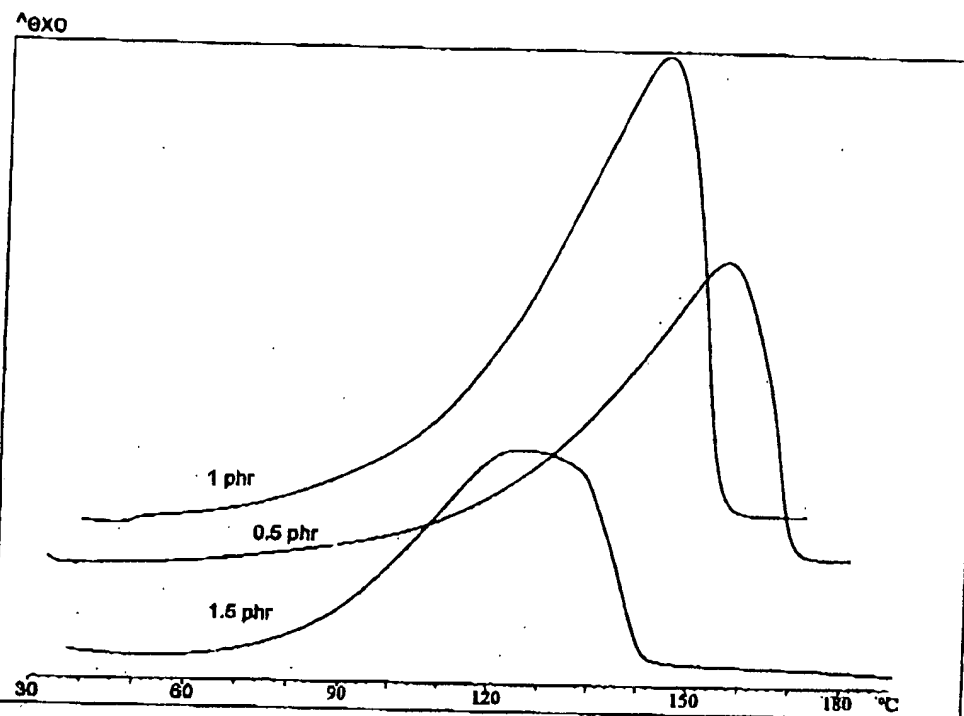


Figure 2. DSC plots of 3,4-epoxycyclohexylmethyl 3,4-epoxycyclohexane carboxylate containing different amounts of lanthanum triflate as catalyst.

coexistence of parallel processes such as chain transfer reactions or depolymerization by "back-biting" to form cyclic oligomers.<sup>[10]</sup> This may change the structure of the network and influence the  $T_g$  values. Moreover, the heat evolved during the coordination of the catalyst to the oxirane ring could influence the value of measured enthalpy.

At the same catalyst percentage (1 phr), the  $BF_3 \cdot MEA$  system does not show a high effectiveness since it leads to an uncured material with a very low  $T_g$  value ( $-19^\circ C$ ). Higher amounts of the catalyst (3 phr) lead to cured material but a  $T_g$  cannot be observed by DSC. However, the enthalpy evolved in this process is significantly lower than for lanthanide triflates.

We also studied how the percentage of the catalyst affects the curing reaction and the thermal characteristics of the crosslinked material. Figure 2 shows the dynamic DSC curves from samples containing different percentages of lanthanum triflate. Higher proportions of the initiator lead to a shift of the peak maximum to lower temperatures. Table 1 collects the thermal parameters of these experiments. Both the onset and the maximum temperatures of the crosslinking decrease when the percentage of initiator increases, whereas the enthalpies and  $T_g$  values are difficult to rationalize. The higher reactivity of cycloaliphatic epoxy resins towards lanthanide triflates makes it unadvisable to use proportions of catalyst greater than 1 phr, because of the heat that evolves in the sample preparation can make their use in some applications difficult.

Technological applications of epoxy resins require the knowledge of time and processing temperature to completely cure the material. The isoconversional kinetic analysis of non-isothermal data is useful for predicting these parameters. Isoconversional kinetic analysis is based on the idea that the reaction rate at a constant conversion depends only on the temperature.

For crosslinking processes as complicated as a cationic curing, which implies back-biting or chain transfer, a isoconversional kinetic analysis provides better predictions than a kinetic analysis based on a single-step kinetic equation. If changes in the mechanism are associated with changes in the activation energy, they can be detected by the model-free isoconversional method.<sup>[11]</sup> This method is used to evaluate the dependence of the activation energy on the degree of crosslinking. Interpreting such dependencies is a useful application of this method.<sup>[12]</sup>

In a previous paper<sup>[3]</sup> we used this method to study the crosslinking of DGEBA with lanthanide triflates. In this paper we have used it to kinetically study the crosslinking of cycloaliphatic epoxy resins with the same type of initiators to compare the behavior of both types of resins.

In Figure 3  $E_a$  is plotted against the conversion degree at different initiator percentages. This method causes the values in the first part of the curve to be highly inaccurate, since the formation of the active initial species may produce a variation in  $E_a$  during the first steps of the reaction. In the last part of the curve a change from kinetic to

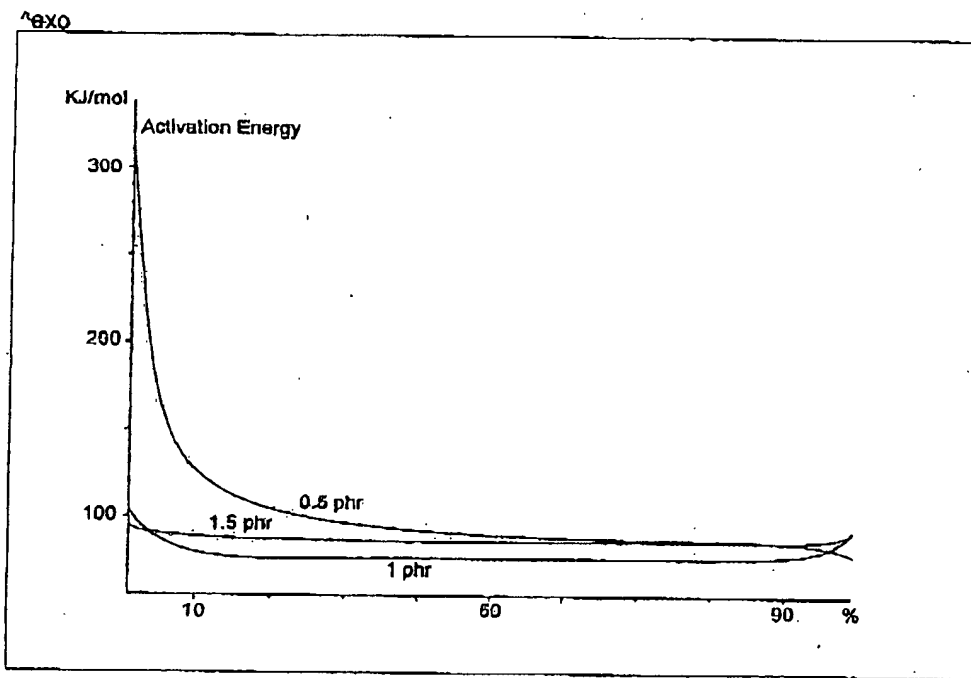


Figure 3.  $E_a$  versus conversion degree for the curing of 3,4-epoxycyclohexylmethyl 3,4-epoxycyclohexane carboxylate with different amounts of lanthanum triflate as catalyst.

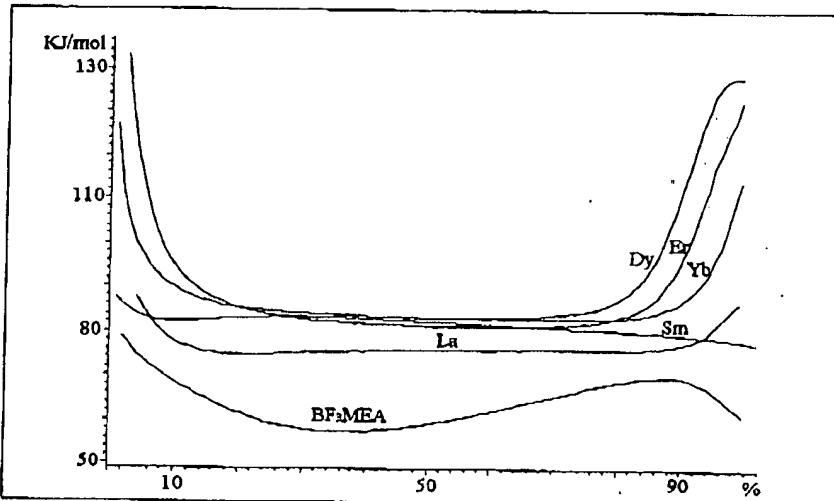


Figure 4.  $E_a$  versus conversion degree for the curing of 3,4-epoxycyclohexylmethyl 3,4-epoxycyclohexane carboxylate with different lanthanide triflates and  $BF_3 \cdot MEA$  as catalysts.

a diffusion-controlled curing can lead to unreliable results above 80% of conversion. As we can see, there are very few differences in the shape of the curves for the different percentages, which indicates that there are no great differences in their mechanisms. The straight line, especially for 1 and 1.5 phr, indicates that there are no changes in the main process in this range. However, it must be mentioned again that higher proportions of catalyst lead to a

reaction at room temperature before the curves can be registered and some information at the beginning of the cure is therefore lost. The  $E_a$  values are very similar (around 80 kJ/mol) and are comparable to those obtained from DGEBA experiments for lanthanum triflates.

Figure 4 shows the curves of  $E_a$  against conversion degrees obtained from each catalyst at 1 phr and from  $BF_3 \cdot MEA$  at 3 phr. The curves for lanthanide triflates

Table 2. Predicted times of curing from isoconversional analysis for the curing of 3,4-epoxycyclohexylmethyl 3,4-epoxycyclohexane carboxylate containing 1 phr of different lanthanide triflates, different amounts of lanthanum triflate and 3 phr of  $\text{BF}_3\text{-MEA}$  as catalysts.

| Catalyst                  | Init.<br>percent.<br>phr | Predicted time of curing in min |       |       |       |
|---------------------------|--------------------------|---------------------------------|-------|-------|-------|
|                           |                          | 80°C                            | 100°C | 120°C | 140°C |
| $\text{Yb}(\text{OTf})_3$ | 1                        | 147                             | 25    | 5     | 1     |
| $\text{Sm}(\text{OTf})_3$ | 1                        | 50.5                            | 12    | 3.5   | 1     |
| $\text{Dy}(\text{OTf})_3$ | 1                        | >600                            | 191   | 21    | 3     |
| $\text{Er}(\text{OTf})_3$ | 1                        | 359                             | 45.5  | 6.5   | 1.5   |
| $\text{La}(\text{OTf})_3$ | 1                        | 85                              | 19.5  | 5     | 1.5   |
| $\text{La}(\text{OTf})_3$ | 1.5                      | 37                              | 8     | 2     | 0.5   |
| $\text{La}(\text{OTf})_3$ | 0.5                      | 265                             | 55    | 13    | 3.5   |
| $\text{BF}_3\text{-MEA}$  | 3                        | 37                              | 12    | 4     | 1.5   |

look similar, while the plot for  $\text{BF}_3\text{-MEA}$  decreases until 30–40% of conversion and increases at higher degrees of conversion. This agrees with the coexistence of different stages with different activation energies in the curing catalyzed with  $\text{BF}_3\text{-MEA}$ .<sup>[13]</sup> The variation of the  $E_a$  with the conversion degrees is not significant for this series of lanthanide triflates. The  $E_a$  values are very close for the triflates, but the lanthanum salt shows a slightly lower value than the others.

We can predict the crosslinking degree from time and temperature of curing via the isoconversional analysis. Table 2 shows the predicted times needed to reach a prac-

tically complete curing at different temperatures for the different lanthanide triflates and  $\text{BF}_3\text{-MEA}$ . The predicted times when different proportions of lanthanum salt were used are also given.

We can see that when 1 phr of the catalyst is used, samarium salt is the most suitable catalyst at low curing temperatures. Dysprosium triflate needs longer times to reach the curing at all the temperatures studied. At 80°C, for example, more than 600 min are necessary. Similarly, the higher the proportion of catalyst the higher the curing rate. Thus, at 80°C only 37 min is necessary to reach the complete crosslinking with 1.5 phr of lanthanum salt. All the catalysts show their best effectiveness at high temperatures (120–140°C). The  $\text{BF}_3\text{-MEA}$  system needs more catalyst to produce a comparable curing rate.

A different reactivity order was found for similar experiments carried out with DGEBA as a resin. For glycidic compounds the highest reactivity at low temperatures was for erbium triflate.<sup>[3]</sup> The different reactivity order for the two resins may be due to the different electronic density of the two oxiranic oxygens. These can lead to a different coordination and a variation in the cationic character in the active species. Similarly, the different coordinative abilities of lanthanide salts produce great variations in the reaction rate. Moreover, these experiments proved that with lanthanide triflates cycloaliphatic epoxy resins are more reactive than conventional DGEBA resins.

Table 3. Predicted and measured times to reach a practically complete curing of 3,4-epoxycyclohexylmethyl 3,4-epoxycyclohexane carboxylate containing 1 phr of different lanthanide triflates, different amounts of lanthanum triflate and 3 phr of  $\text{BF}_3\text{-MEA}$  as catalysts.

| Catalyst                  | Init. percent.<br>phr | Temperature<br>°C | Time<br>min | Experimental<br>crosslinking degree |    | Predicted<br>crosslinking degree<br>% |
|---------------------------|-----------------------|-------------------|-------------|-------------------------------------|----|---------------------------------------|
|                           |                       |                   |             | %                                   | %  |                                       |
| $\text{Yb}(\text{OTf})_3$ | 1                     | 80                | 11          | 25                                  | 75 | 25                                    |
|                           |                       | 100               | 12          |                                     |    | 75                                    |
|                           |                       | 120               | 4           |                                     |    | 90                                    |
| $\text{Sm}(\text{OTf})_3$ | 1                     | 80                | 6           | 26                                  | 75 | 25                                    |
|                           |                       | 100               | 8           |                                     |    | 75                                    |
|                           |                       | 120               | 3           |                                     |    | 90                                    |
| $\text{Dy}(\text{OTf})_3$ | 1                     | 80                | 6           | >95                                 | 90 | 10                                    |
|                           |                       | 100               | 11          |                                     |    | 50                                    |
|                           |                       | 120               | 11          |                                     |    | 90                                    |
| $\text{Er}(\text{OTf})_3$ | 1                     | 80                | 11          | 25                                  | 75 | 25                                    |
|                           |                       | 100               | 12          |                                     |    | 75                                    |
|                           |                       | 120               | 5           |                                     |    | 90                                    |
| $\text{La}(\text{OTf})_3$ | 1                     | 80                | 11          | 27                                  | 75 | 25                                    |
|                           |                       | 100               | 12          |                                     |    | 75                                    |
|                           |                       | 120               | 5           |                                     |    | 90                                    |
| $\text{La}(\text{OTf})_3$ | 1.5                   | 80                | 11          | 56                                  | 75 | 50                                    |
|                           |                       | 100               | 5           |                                     |    | 75                                    |
|                           |                       | 120               | 2           |                                     |    | 95                                    |
| $\text{La}(\text{OTf})_3$ | 0.5                   | 80                | 20          | >95                                 | 95 | 10                                    |
|                           |                       | 100               | 20          |                                     |    | 50                                    |
|                           |                       | 120               | 12          |                                     |    | 90                                    |
| $\text{BF}_3\text{-MEA}$  | 3                     | 80                | 8           | 22                                  | 75 | 25                                    |
|                           |                       | 100               | 7           |                                     |    | 75                                    |
|                           |                       | 120               | 4           |                                     |    | 95                                    |

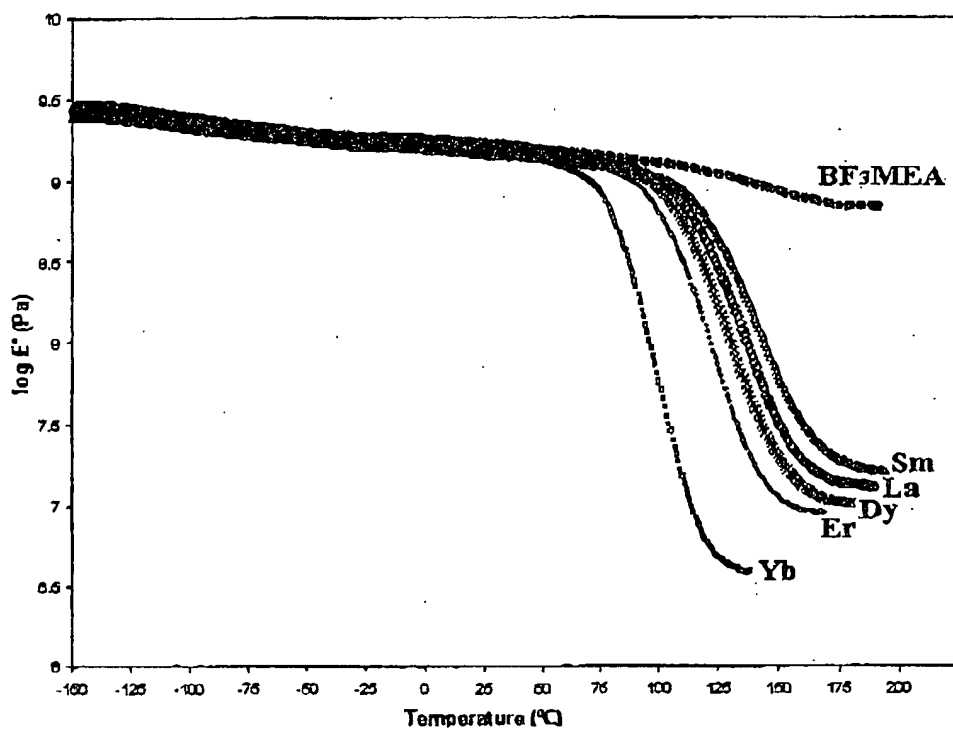


Figure 5. Storage modulus ( $E'$ ) as a function of temperature for the cured 3,4-epoxycyclohexylmethyl 3,4-epoxycyclohexane carboxylate with the different catalysts.

To test the accuracy of the isoconversional analysis in predicting the curing conditions, we performed isothermal experiments at different temperatures and times. Isothermal scans of samples containing different catalysts were recorded for selected times. Then, in a second dynamic scan we evaluated the residual enthalpies. By comparing these enthalpies with those in Table 1, we calculated the curing degrees achieved in the isothermal scans. Table 3 shows the experimental and predicted curing degrees at different conditions for all the catalysts. The good agreement between these values indicates the accuracy of the isoconversional method for making predictions in this range. The shape of the curve in the  $\text{BF}_3 \cdot \text{MEA}$  system made it impossible to prove the agree-

ment between the predicted and the experimental degree of curing at  $120^\circ\text{C}$ , since the residual enthalpy could not be accurately evaluated.

Dynamic mechanical analyses of the cured samples were made to study the effects of curing initiators on the morphology of the network formed and on the viscoelastic and mechanical properties.

In Figure 5 the storage modulus,  $E'$ , is plotted versus temperature for the different lanthanide triflates. The storage modulus indicates the stiffness and elastic behavior of the materials. We can see that the drop of  $E'$  from the unrelaxed states to the relaxed states is not the same for all samples. The reference system with  $\text{BF}_3 \cdot \text{MEA}$  used as a reference, behaves in a completely different way.

Table 4. DMTA data obtained from 3,4-epoxycyclohexylmethyl 3,4-epoxycyclohexane carboxylate containing 1 phr of different lanthanide triflates, different amounts of lanthanum triflate and 3 phr of  $\text{BF}_3 \cdot \text{MEA}$  as catalysts.

| Catalyst                  | Init. percent.<br>phr | Ionic radii<br>Å | Maximum peak<br>temperature tan $\Delta\beta$ ( $T_{M\beta}$ )<br>°C | Maximum peak<br>temperature tan $\Delta\alpha$ ( $T_{M\alpha}$ )<br>°C | Molecular weight<br>between crosslinks $M_c$ |
|---------------------------|-----------------------|------------------|--|--|--|
| $\text{Yb}(\text{OTf})_3$ | 1                     | 0.858            | -72  | 82   | 3 198  |
| $\text{Sm}(\text{OTf})_3$ | 1                     | 0.964            | -85  | 120  | 726  |
| $\text{Dy}(\text{OTf})_3$ | 1                     | 0.908            | -58  | 108  | 1 153  |
| $\text{Er}(\text{OTf})_3$ | 1                     | 0.881            | -79  | 100  | 1 420  |
| $\text{La}(\text{OTf})_3$ | 1                     | 1.061            | -76  | 113  | 921  |
| $\text{La}(\text{OTf})_3$ | 1.5                   | -                | -71  | 88   | 1 355  |
| $\text{La}(\text{OTf})_3$ | 0.5                   | -                | -78  | 81   | 2 014  |
| $\text{BF}_3\text{MEA}$   | 3                     | -                | -74  | 147  | -  |

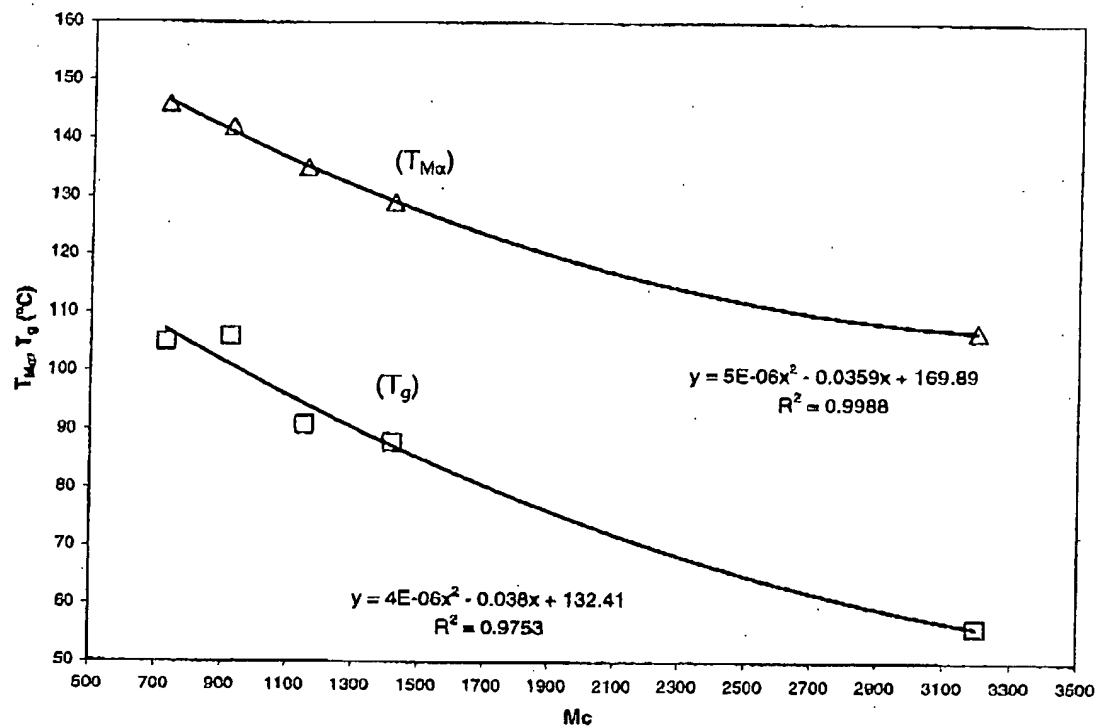


Figure 6. Plot of the correlation of  $T_{Ma}$  and  $T_g$  versus  $M_c$  for the cured 3,4-epoxycyclohexylmethyl 3,4-epoxycyclohexane carboxylate with the different lanthanide triflates as catalysts.

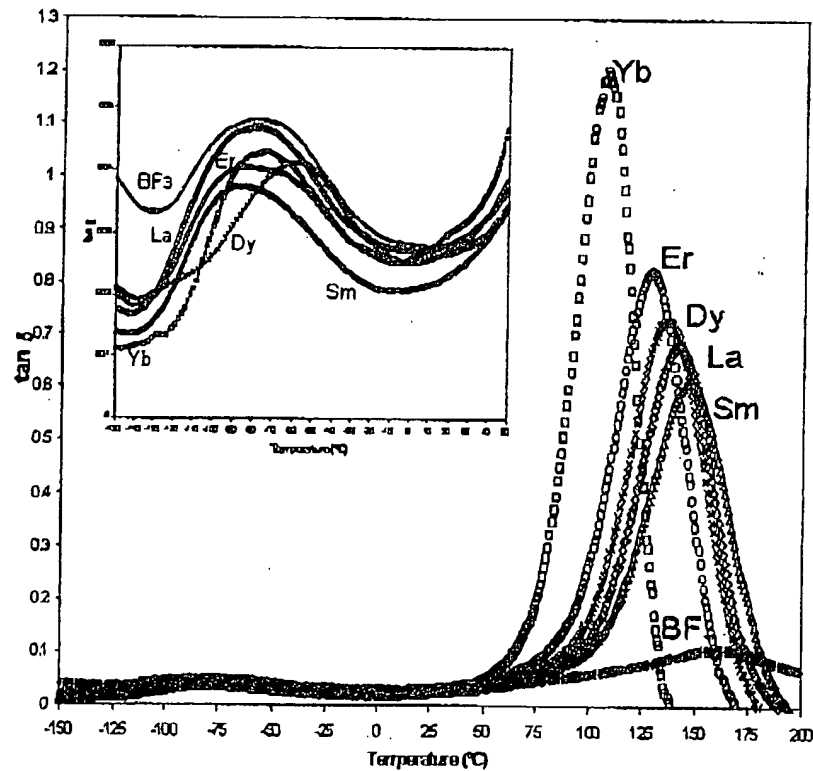


Figure 7. Plot of loss factor ( $\tan \delta$ ) as a function of temperature of the cured 3,4-epoxycyclohexylmethyl 3,4-epoxycyclohexane carboxylate with all catalysts. Inset: Expansion of the -150–50 °C temperature range.

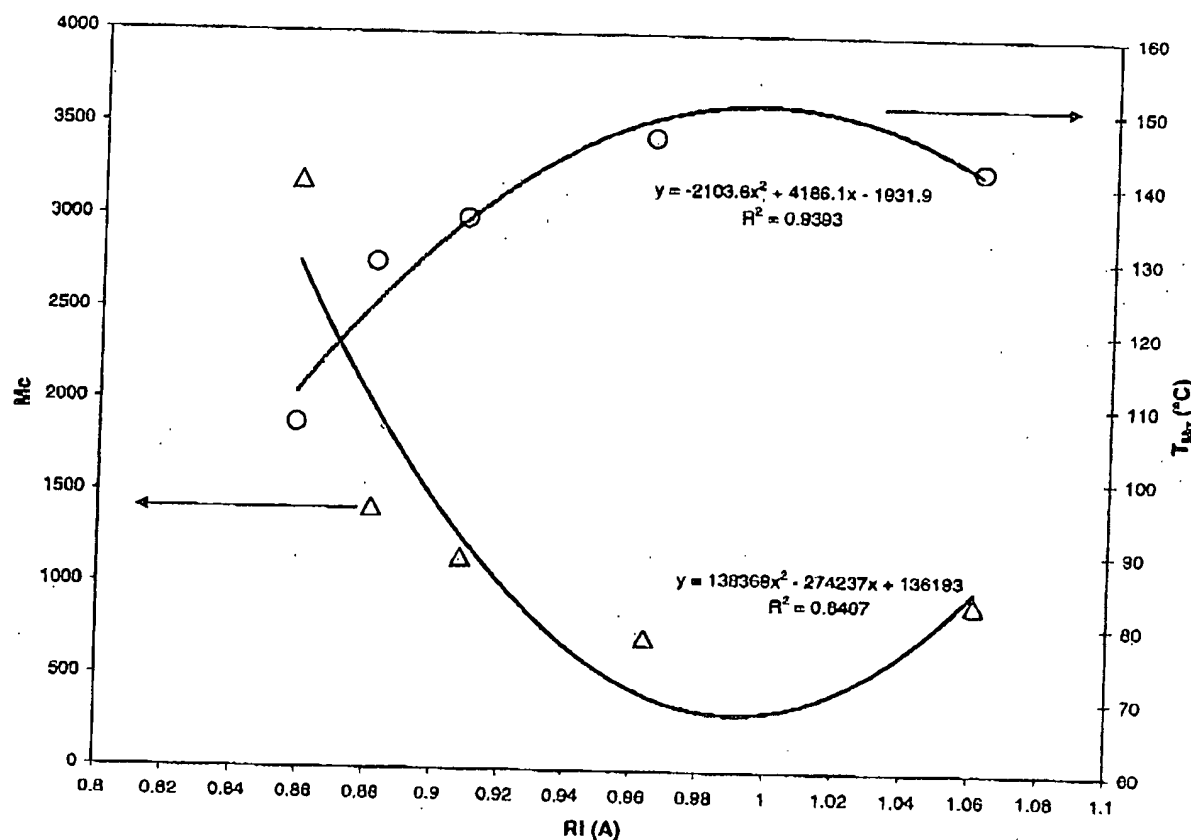


Figure 8. Plot of  $M_c$  and  $T_{ma}$  of the cured 3,4-epoxycyclohexylmethyl 3,4-epoxycyclohexane carboxylate versus atomic radii of the different lanthanide ions.

From the theory of rubber elasticity<sup>[14]</sup> and using the modulus of relaxed material ( $E'_r$ ) we can calculate the molecular weight between crosslinks ( $M_c$ ) by applying the simplified equation:

$$M_c = \frac{3\phi \delta RT}{E'_r}$$

where  $\phi$  is the front factor (considered in this work,  $\phi = 1$ ),  $\delta$  is the density of the sample,  $T$  the Kelvin temperature and  $R$  the universal gas constant.

Table 4 shows the values of  $M_c$  obtained from the modulus of relaxed samples for the different initiators used, estimated at the temperature of the  $\alpha$ -peak plus 30°C. Figure 6 shows that there are good correlations between the  $M_c$  and the temperature of the maximum of  $\alpha$ -transition peak ( $T_{Ma}$ ) and between the  $M_c$  and the DSC glass transition temperature (see Table 1). As usual, the  $T_{Ma}$  are higher than the  $T_g$  values due to a different definition of glass transition and the experimental differences in the transition from the glassy to the rubbery states.  $T_{Ma}$  of the different samples in Table 4 were obtained from the experimental spectra of the loss tangent ( $\tan \delta$ ) versus the temperature (Figure 7).

Figure 7 shows that, besides the  $\alpha$ -transition peak, all the samples exhibit another broad peak, which in the literature is called the  $\beta$ -relaxation. The  $\alpha$ -relaxation curve is associated to the long-range segmental motions of the network and to the glass transition temperature phenomena. Most authors associate the  $\beta$ -relaxation with restricted molecular segmental motions.<sup>[15,6]</sup> The differences between the shapes of the  $\alpha$  and  $\beta$  peaks of the samples obtained from the different initiators with the values of the  $M_c$  obtained indicate that, although all triflate initiators produce apparently full cured epoxy resins, the crosslinked structures and the networks formed are not the same. Samarium triflate produces the highest crosslinked material and ytterbium triflate produces the lowest.

We believe that the molecular volume of the initiator may affect the crosslinked structures of the cured samples and explain the different behaviors. Figure 8 shows the degrees of correlation between the radii of metallic ion, obtained from the literature<sup>[17]</sup> of the triflate initiators, and the maximum of the  $\alpha$ -transition peak, and the molecular weight between crosslinks,  $M_c$ . These correlations are rather good, especially with the  $T_{Ma}$ . The maximum and minimum that appear in the correlations suggest an optimum molecular volume of the triflate initiator.

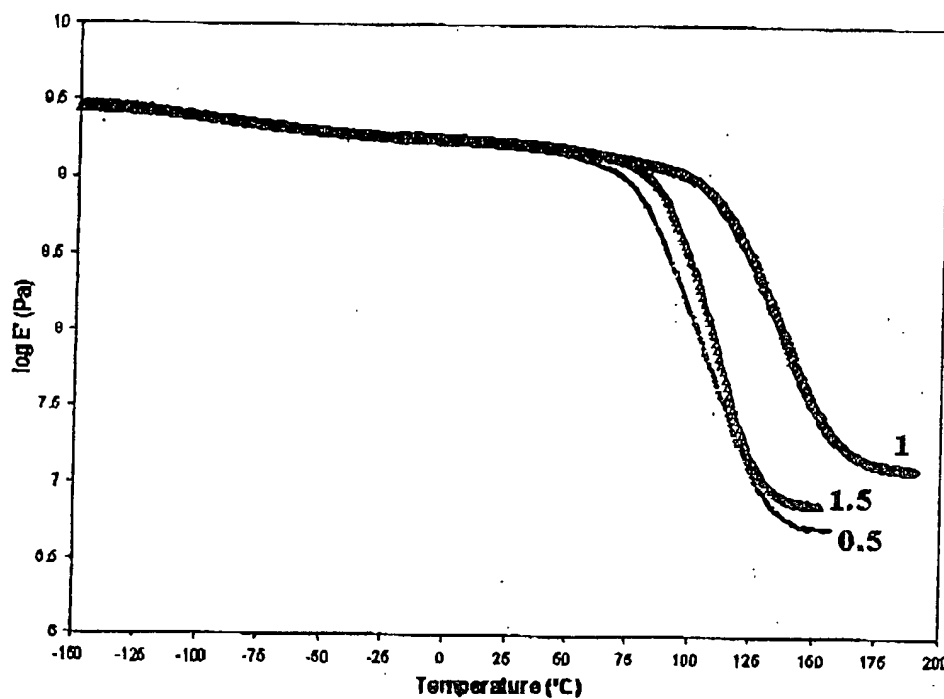


Figure 9. Storage modulus  $E'$  of cured 3,4-epoxycyclohexylmethyl 3,4-epoxycyclohexane carboxylate with different amounts of lanthanum triflate as catalyst versus temperature.

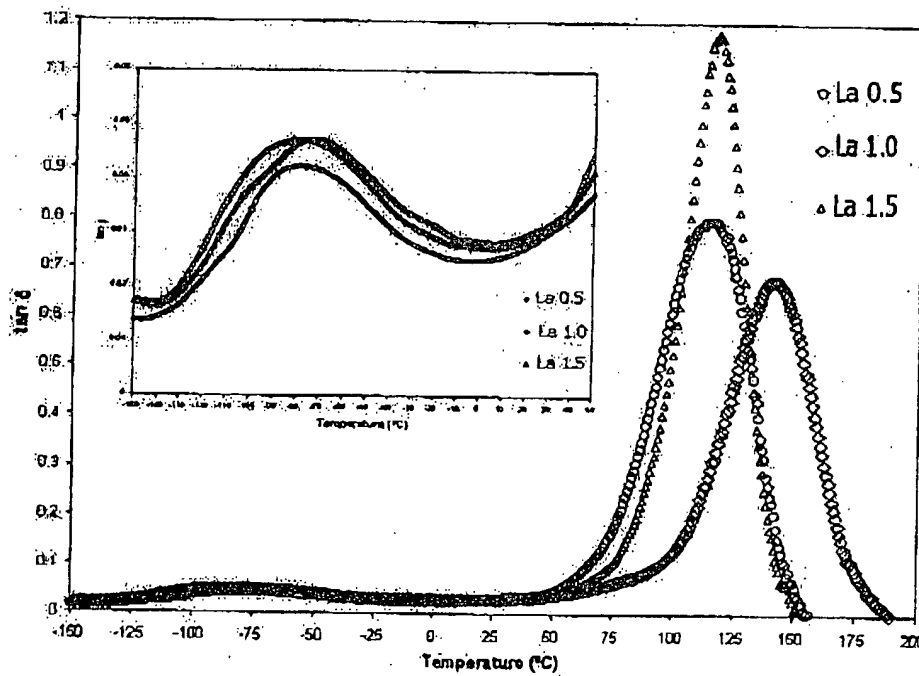


Figure 10. Plot of loss factor ( $\tan \delta$ ) as a function of temperature of the cured 3,4-epoxycyclohexylmethyl 3,4-epoxycyclohexane carboxylate with different amounts of lanthanum triflate. Inset: Expansion of the -150–50 °C temperature range.

Figure 9 and 10 show the storage moduli  $E'$  and the loss tangent  $\tan \delta$ , of samples with different proportions

of lanthanum triflate. The proportion of catalyst influences both parameters. Results are best with 1 phr of

initiator; lower and higher proportions produce a material with lower glass-transition temperature and poorer cross-linked networks.

To sum up, we have proved that lanthanide triflates are good candidates for crosslinking cycloaliphatic epoxy resins when used at a proportion of 1 phr. From all of these, samarium triflate leads to the highest crosslinked material, even at the lowest temperatures. This good behavior seems to be related to the ionic radius of this metal.

Also, isoconversional kinetic analysis is a good tool for predicting the suitable reaction conditions for a complete crosslinking.

**Acknowledgement:** The authors would like to thanks the DGI-CYT (Dirección General de Investigación Científica y Tecnológica) PB99-0520 and CIRIT (Comissió Interdepartamental de Recerca i Innovació Tecnològica) 98SGR 00097 for providing financial support and to PETRI.

Received: August 24, 2000

Revised: December 4, 2000

- [1] T. Endo, F. Sanda, *Macromol. Symp.* **1996**, *107*, 237.
- [2] S. Kobayashi, *Synlett* **1994**, 689.
- [3] P. Castell, M. Galià, A. Serra, J. M. Salla, X. Ramis, *Polymer* **2000**, *41*, 8465.
- [4] M. D. Soucek, O. L. Abu-Shanab, C. D. Anderson, S. Wu, *Macromol. Chem. Phys.* **1998**, *199*, 1035.
- [5] C. A. May, "Epoxy Resins. Chemistry and Technology", 2nd ed., Marcel Dekker, Inc., 1988.
- [6] K. Morio, H. Murase, H. Tsuchyalla, T. Endo, *J. Appl. Polym. Sci.* **1986**, *32*, 5727.
- [7] J. V. Crivello, U. Varleman, *J. Polym. Sci., Part A: Polym. Chem.* **1995**, *33*, 2463, *ibid.* **1995**, *33*, 2473.
- [8] M. Tokizawa, H. Okada, N. Wakabayashi, *J. Appl. Polym. Sci.* **1993**, *50*, 875.
- [9] H. Lee, K. Neville, "Handbook of Epoxy Resins", McGraw-Hill, New York 1967.
- [10] D. J. Brunelle, "Ring Opening Polymerization", Hanser Publishers, Passau 1993.
- [11] S. Vyazovkin, N. Sbirrazzuoli, *Macromolecules* **1996**, *29*, 1867.
- [12] S. Vyazovkin, N. Sbirrazzuoli, *Macromol. Rapid Commun.* **1999**, *20*, 387.
- [13] Y. Li, M. Li, F. Chang, *J. Polym. Sci., Part A: Polym. Chem.* **1999**, *37*, 3614.
- [14] A. V. Tobolsky, D. W. Carlson, N. Indictor, *J. Polym. Sci.* **1960**, *54*, 175.
- [15] L. C. E. Struik, *Polymer* **1987**, *28*, 57.
- [16] M. Ochi, M. Yoshizumi, M. Shimbo, *J. Polym. Sci., Polym. Phys. Ed.* **1987**, *25*, 1817.
- [17] R. C. Weast, Ed., "Handbook of Chemistry and Physics", CRC Press, Cleveland 1972, F-177.